

Research Article

Study on Roof Presplitting Mechanism and Deformation Control of Reused Roadway in Compound Soft Rock by Roof Presplitting Approach

Fuzhou Qi ¹, Dangwei Yang ^{2,3}, Xinming Li,¹ Bin Li,¹ Yingying Zhai,¹ and Shuisheng Yu ¹

¹School of Civil & Architecture Engineering, Zhongyuan University of Technology, Zhengzhou, 450007 Henan, China

²Pingdingshan University, Pingdingshan, 467000 Henan, China

³Pingdingshan Coal No. 10 Mine, Pingdingshan, 467000 Henan, China

Correspondence should be addressed to Dangwei Yang; ydw15162171009@163.com

Received 27 December 2021; Accepted 11 July 2022; Published 1 August 2022

Academic Editor: Hualei Zhang

Copyright © 2022 Fuzhou Qi et al. This is an open access article distributed under the Creative Commons Attribution License, which permits unrestricted use, distribution, and reproduction in any medium, provided the original work is properly cited.

Based on the compound soft rock movement law, the rock formation structural features for a mining roadway were examined. Furthermore, the presplitting, extension, and coalescence mechanism of rock formation and the engineering needs for reusing an abandoned underground roadway were studied. According to engineering and geological conditions, an analytic expression of the inertial force, the moment of inertia, and the vertical stress acting on the breakage are obtained by constructing a structural mechanical model of the overlying strata. The transfixion law, the tensile shear failure characteristics, the release rate in the fracture expansion process of presplitting fissures, and the evolution law of the plastic zone in reused roadway surrounding rock on conditions of 0 m, 0.5 m, 1 m, 1.5 m, and 2 m fissure intervals are analyzed by creating a three-dimensional numerical model. The stress distribution and deformation laws of the roadway under mining disturbance are obtained. The results show that when the fissure interval is 1 m, the peak value of the horizontal stress reaches 10~12 MPa, and the stress concentration factor is 1.8~2.2, which promotes fracture expansion and transfixion and controls plastic damage development on both sides of a fracture. The elastic strain energy of the reused roadway is reduced to 32.7% of the peak value. The deformation of the roof is coordinated and deformed. It is helpful for the compound soft rock strata to fall and plug the area, forming a stable composite reused roadway surrounding the rock structure. A 1 m presplitting fissure interval is adopted for field testing, and the monitoring results show that 0~3.0 m behind the mining face, presplitting fissures will be connected and begin to fall. Moreover, 3.0~6.0 m behind the mining face, compound soft rock strata will fall and plug the area fully, forming a reused roadway structure. Severe deformation of reused roadway was reduced, and the stability of surrounding rock was improved by implementing the roof presplitting approach.

1. Introduction

In China, coal resources are dominated by underground mining and result in large abandonment problems in underground spaces such as roadways or underground chambers. These areas are of widespread concern while satisfying the rapid development of social economy requirements. Abandoned underground spaces waste resources and bring hidden dangers such as water bursts, gas outbursts, and strong

mine pressures [1–3]. For the resource development of adjacent areas, a series of environmental problems such as ground subsidence may also occur. Therefore, it is undoubtedly the best solution to solve the above problems by taking full advantage of existing abandoned underground spaces according to local conditions to perform afterheat reuse of the abandoned underground spaces [4, 5]. The abandoned underground spaces of mines include two parts: the leftover and abandoned roadways of the production mine and the

underground mine chamber. Mines are equipped with production systems such as transport, aeration, and pedestrian conditioning systems. Use of the abandoned underground space will more effectively take full advantage of the service functions of every mine production system on the basis of good production and safety. The abandoned roadway and chamber systems in the last mining section can be used as a warehouse for storing production materials or a provisional substation, and water storage increases the use ratio of resources and the length of mine service and reduces environmental pollution. Reused roadways are different from the general mining roadways in that one side lateral wall of the reused roadway is coal-rock mass, while another side is gob, which includes large deformations in the surrounding rock. The superimposed stress of double roadway mining and the adjacent slope is held up by the gob, supporting tremendous mine ground pressure, and is extremely complicated engineering technology [6, 7]. The stability of the surrounding reused roadway rock depends on the degree of stress concentration during mining, and the stress concentration also depends on factors such as the top and bottom mining coal seam slate structure and its mechanical properties and the roof structure after caving. To ensure the stability of the surrounding reused roadway rock, the supporting design and high safety factor and the size and strength enhancing the support inside or adjacent to the roadway are generally adopted [8]. The expected effect is hard to achieve due to the influence of normal production and safety, and they cause unnecessary economic losses [9]. Meanwhile, coal seams with a compound soft roof are widely found; each rock formation is small in thickness with joint and fracture development. There are weak bond forces and low overall strength among rock formations and lower overall strength, so separation rock formations become larger under the surrounding rock pressure. The pressure could easily cause inbreak, and it is hard to form a bearing structure. Thus, there are greater stability requirements for the surrounding reused roadway rock [10, 11].

To solve the above problems, automatic broken roof stowboard technology is developed from compound soft rock, which simplifies the retained roadway technique, improves the retained roadway efficiency, and provides reliable technical support for taking full advantage of the remaining abandoned underground space. In the above technical system, the advance presplitting of the roof formation is an important step [12, 13], since continuous advanced presplitting of the roof on one side of the roadway along with the mining side is required, and the length of the presplitting fissure is up to 1,000 meters. Meanwhile, the influence on mining must be taken into consideration. Thus, there are stringent requirements on the time and structure of advanced presplitting. As a key parameter of roof presplitting, the presplitting fissure intervals have a significant influence on the stress distribution of the roadway surrounding rock, the roof cutting result, and the falling position and state [14]. The intervals become a key factor of whether the reused roadway plays a normal role. In the paper, the 5# coal seam with a compound soft rock roof of the mining area in Linfen, Shanxi, was selected to study the propagation

and coalescence effect of rock presplitting fissure and the stress and deformation law of surrounding rock. Additionally, the plastic zone distribution characteristics of the reused roadway presplitting rock fissure under different presplitting rock fissure intervals were analyzed to provide a basis for the stability of the surrounding reused roadway rock.

2. Study on the Reused Roadway Stratum Structure

2.1. Engineering Background. The coal seam 5# at a mine has an average thickness of 2 m, belonging to medium-thickness coal seams. As shown in the geology columnar Figure 1, the immediate roof stratum of the coal seam is black mudstone with the average thickness of 3.3 m, weak carrying capacity, and crushing and abscission of strata are liable to occur. The main roof stratum is sandy mudstone with the average thickness of 3.1 m, with good stability, and having direct impact on the roadway pressure. The main roof stratum has sandy mudstone with the average thickness of 7.7 m at the top. The overlying rock of coal seam 5# is the thick-stratum soft compound rock strata, mainly mudstone strata and sandy mudstone strata. It has low strength and weak carrying capacity. Under the effect of mining disturbance, fracture development and severe deformation may occur (Figure 2), so the roadway is hard to maintain. In order to make full use of abandoned roadway in the 5203 mining face, the air return roadway of the 5203 mining face as air return roadway is near the 5205 working face, and the transport roadway for the production material storage warehouse is in 52 mining section.

2.2. Analysis of Presplitting Structure of Composite Soft Rock Strata. The gob side of the compound soft rock roof is broken to cut the connection of the roadway roof and the overlying rock on the gob side. This process also shortens the hanging length of the roof rock beam at the roadway gob and weakens the superimposed pressure caused by mining disturbances. Meanwhile, under the effect of its own gravity, the overlying rock pressure, and the mining disturbance, the compound soft rock strata will be cut along the presplitting fracture. Using the bulking collapsed rock characteristics, the roadside gob is filled to form the retained roadway of the gangue wall, and contact is made with the overlying stable rock. The bearing structure is formed at the area of gob side to support the overlying rock pressure and form a coordinated control structure of the roadway surrounding rock by “roof breaking+pressure releasing+filling with collapsed rock,” as shown in Figure 3.

The roof presplitting will weaken the boundary constraint of A, as shown in Figure 3(a).

The curvature of the compound soft rock formation group axis after deformation appeared as follows [15]:

$$\frac{1}{\rho} = \frac{M_0}{EI_z}. \quad (1)$$

M_0 is the bending moment of the compound soft rock under the mine pressure effect, E refers to the rock formation elasticity modulus, and I_z is the rock formation inertia

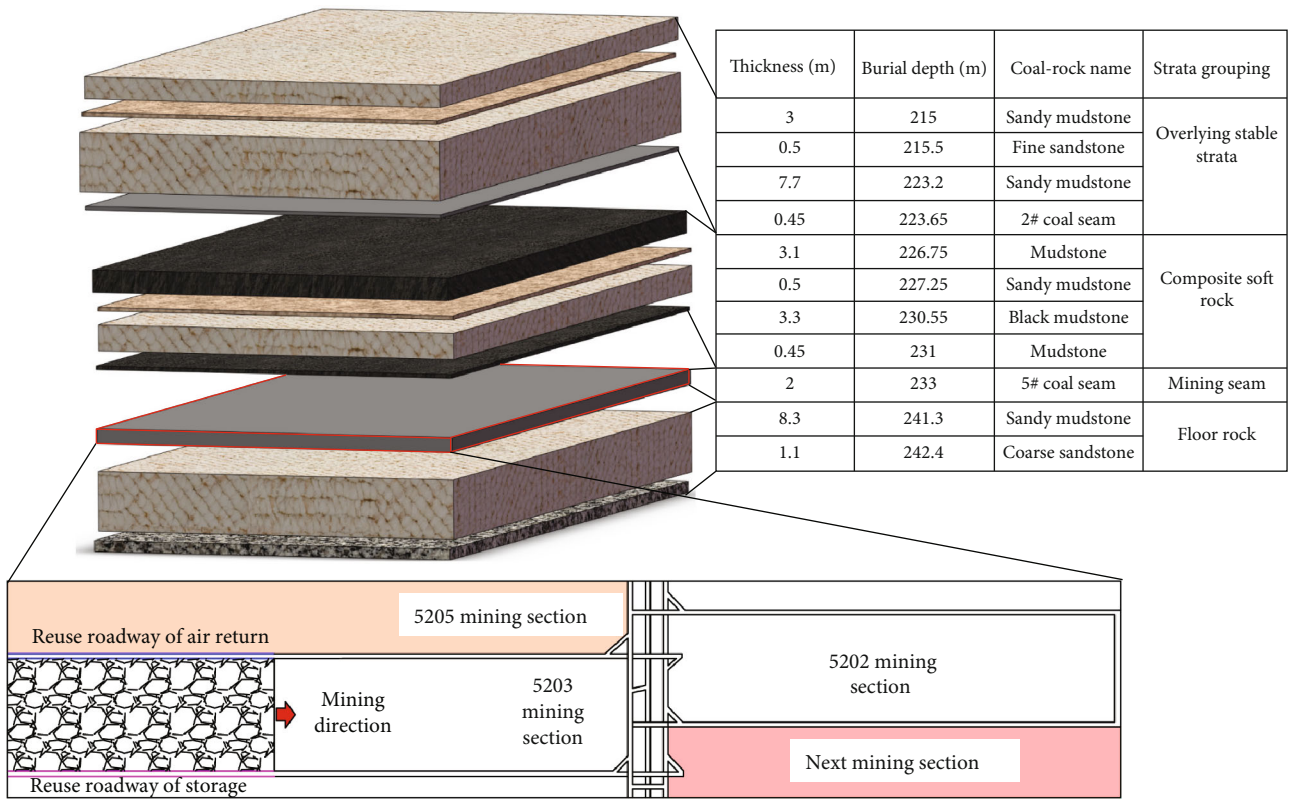


FIGURE 1: Geological structure of strata.

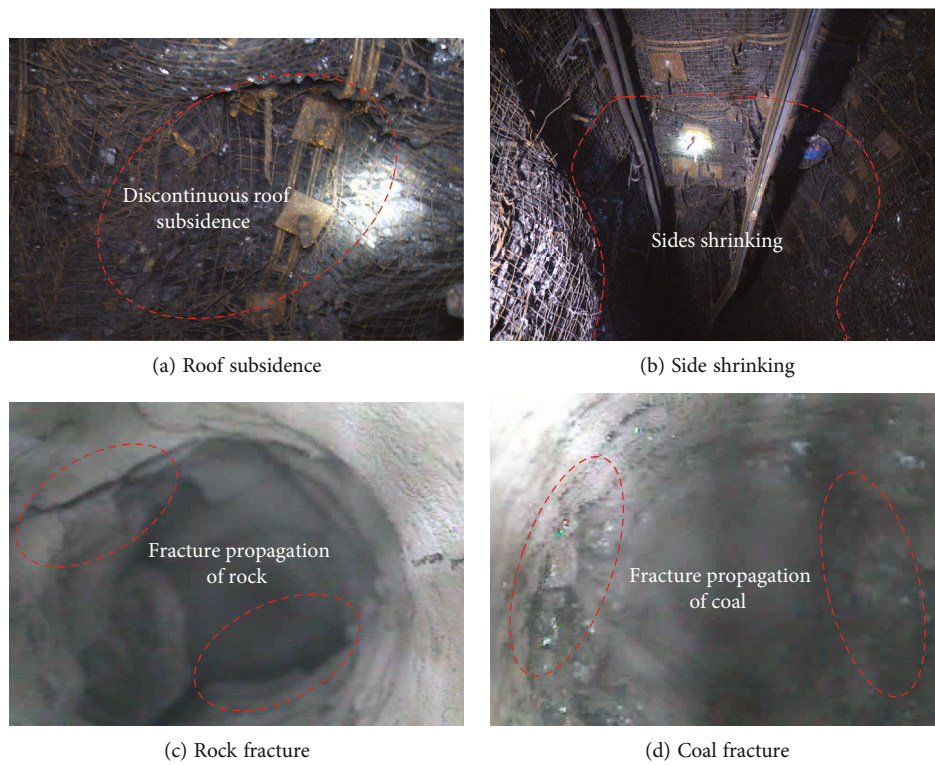


FIGURE 2: Failure mode of soft roadway.

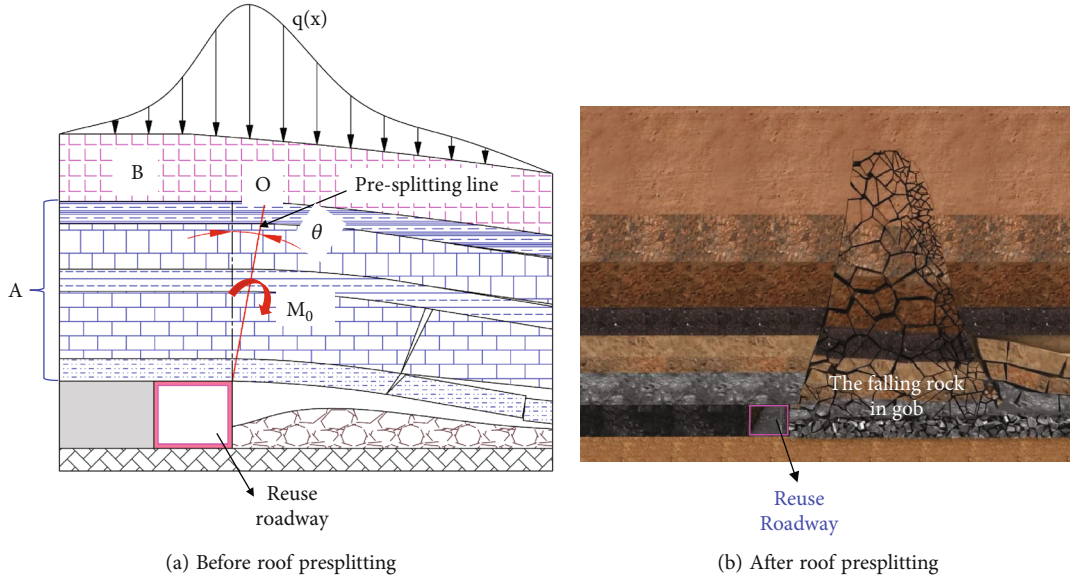


FIGURE 3: Mechanical model of the presplitting structure of compound soft rock strata.

moment; among them, EI_z is the flexural rigidity of the rock formation. At the time of rock formation presplitting, the roof flexural rigidity EI_z reaches a maximum; as the presplitting fissure interval decreases, the controlling effects of the surrounding rock formation on the gob roof formation diminish, the sinking bending becomes obvious, the curvature increases, and when the presplitting fissure interval is 0, that is, when the presplitting fissure is mutually connected, the flexural rigidity is minimal. If the weakening degree of the rock formation flexural rigidity after presplitting is large, M_0 drops rapidly, and compound soft rock will undergo drastic bending, subsidence, and reversal falling. The lower rock formation as well as the overlying and comparatively complete rock formation cannot deform synchronously and coordinately, or the dynamic loading effect will occur and threaten the surrounding roadway rock stability. If the weakening degree of the rock formation flexural rigidity after presplitting is small, the compound soft rock cannot break along the fissure in time, the roof exposed area increases, the stress concentration occurs on the solid coal-rock side of the roadway, and the plastic damage scope of the surrounding rock increases. Hence, the optimizing fissure width parameter can control the rock formation structure, the caving position, and the presplitting roof state; improve stress conditions of the roadway surrounding rock; and ensure the stability of the reused roadway.

The compound soft rock strata fall along the presplitting fissure and form the supporting structure in the gob side of the reused roadway, as shown in Figure 2(b). The upper stable rock B will rotate and bend at point O , and the support strength of the filling support structure for the high top plate B is as follows [16, 17]:

$$E \cdot (l - a) \cdot \sin \theta = P_0, \quad (2)$$

where E is the caving gangue supporting elasticity modulus; P_0 is the loose gangue strength; θ is the upper rock forma-

tion angle; l is the suspended roof length, basically being the same as that of the periodic fracture of the rock stratum and could be monitored on field; and a is the roadway width. It is known from Equation (2) that when the angle is larger, the holding power borne by the filled rubble is larger, and the cantilever beam caves easily on the kerf after presplitting, which effectively reduces the acting force of the upper rock formation bending deformation on the caving support and enhances the stability of the reused roadway surrounding rock structure.

I_B is the moment of inertia of the upper stable rock B . l_B is the hanging length of rock B on the gob side. α_0 is the rotational acceleration of rock B . The inertia force F_B and inertia moment of couple M_B acting on the base point O are [18, 19]

$$F_B = m\alpha_0 = m \frac{l_B}{2} \alpha, \quad (3)$$

$$M_B = J_B \alpha = \frac{1}{3} m l_B^2 \alpha,$$

where $\alpha_0 = (L/2)\alpha$ and $q(x)$ is the equation of vertical load distribution for rock B and is the vertical shear stress of the key block B at the gob side. According to the force balance in the vertical direction, the vertical force F_O acting on B at O point is

$$F_O = f_o + \int_0^l q(x) dx + mg - \frac{\alpha m l_B}{2}. \quad (4)$$

Therefore, when the compound soft rock strata are falling, the dynamic pressure of the upper strata B causes the rapid pressurization of the support structure collapse and is one of the key factors affecting the stability of surrounding rock of the reused roadway.

2.3. Determination of Roof Breaking Height. The height of rock stratum caving after compaction will depend on the bulking coefficient K_p of the rock. The rock caving at the roof soft rock caving zone in the working face is irregular. After recompaction, the loosening coefficient is low and the residual breaking expansion coefficient K_p is taken as 1.2 [20]. When the caving thickness of the overlying rock stratum is $\sum h$, the accumulation height after caving is $K_p \sum h$. The possible gap remaining with the overlying stable rock stratum is [21, 22]

$$\Delta = \sum h + M - K_p \sum h = M - \sum h(K_p - 1), \quad (5)$$

where M is the mining height, taken as 2 m, and K_p is the residual bulking coefficient of rock, taken as 1.2.

According to Equation (5), when $M = \sum h(K_p - 1)$, $\Delta = 0$, i.e., the falling overlying rock will fill up the gob to support the load of overlying rock. Thus, the required thickness of the overlying rock to fill up the gob is

$$\sum h = \frac{M}{K_p - 1}. \quad (6)$$

The parameters are entered into Equation (6) to obtain $\sum h$. For the 5203 panel, the coal seam mining height is 2 m, and the height of the caved zones is 9.9 m based on field measurement. According to above equation, the bulking coefficient is 1.2 and the fracturing height of the roof strata is 10 m.

3. Analysis of the Presplitting Fissure Extension and Presplitting Roof Stability

3.1. Model Establishment. According to the field monitoring results, the effective fracture length is 2 m. In order to study the migration law and the presplitting effect of the roof rock under different presplitting fissure intervals, the continuous element numerical model is established for the presplitting fissure intervals of 0, 0.5 m, 1 m, 1.5 m, and 2 m, respectively. Ahead of the presplitting with the mining at the same time, the establishment of the model is shown in Figure 4.

m, n, φ , and h , respectively, are for the resplitting length, intervals, deflection angle, and height. The direction of m, n is consistent with the mining direction of the 5203 working face in the numerical model.

The size of model is 85 m \times 45 m \times 37 m. The equivalent load is applied to the upper boundary of the model. The lateral displacement of the model is limited, and the vertical movement is restricted by the bottom surface. The Mohr-Coulomb strength criterion is used to judge the yielding state of coal and rock mass [23, 24]:

$$f_s = \sigma_1 - \sigma_3 \frac{1 + \sin \varphi}{1 - \sin \varphi} + 2C \sqrt{\frac{1 + \sin \varphi}{1 - \sin \varphi}}, \quad (7)$$

where σ_1 and σ_3 are the maximum and minimum main stress, respectively. C and φ are the bonding force and fric-

tional angle of the rock, respectively. When $f_s > 0$, the material will experience shear failure, according to the law of tensile strength ($\sigma_3 \geq \sigma_t$) to analyze whether there is rock tensile deformation. See Table 1 for the physical and mechanical parameters of the rock stratum. In the numerical model, before extraction of the 5203 panel, a roof presplitting line is arranged in the roof strata of reused roadway. This was performed by adopting null element representing the roof fracturing line.

3.2. Distribution Horizontal Stress Characteristics. The presplitting fissure is an opening-type fracture that induces the roof rock formation to extend and cut along the predetermined direction. The superimposed stress caused by mining disturbance plays a leading role on the presplitting fissure extension [25]. Under static-dynamic loading, the fissure tip stress is concentrated. When the horizontal stretching stress of the rock formation on both sides of the fissure exceeds the extension strength of the rock formation, the rock formation will break along the fissure tip and the compound soft roof on the gob side will experience large horizontal displacement. The bearing capacity of the sandy mudstone at 0.5-3.5 m above the reused roadway is strong, which is close to the roadway and has a strong control effect on the caving of the compound soft rock formation. The average breaking distance period of intact rock formations is 25-30 m. The slice at 3 m above the reused roadway is taken as the main object of study in the model, and the survey line is set at 2 m away from the presplitting fissures in the roadway. Figure 5 shows the horizontal stress nephogram for both sides of the presplitting fissures and the horizontal stress curve at the survey line.

The development and coalescence of the presplitting fissure are accompanied by the stress evolution of rock mass around the fracture. Figure 5 shows a presplitting interval of 0 m, and the presplitting fissures coalesced in the initial section of the retained roadway. When mining 0-6 m, the rock with presplitting fissures is in an unstable state because the roof loses the binding force on one side. The surrounding horizontal stress is then concentrated in the ends of the fracture, and the horizontal stresses reaches 8-12 MPa, while the stress concentration factor is 1.45-2.18. When mining to 6-9 m, the horizontal tensile stress is drastically attenuated from the peak and remains stable. The average horizontal tensile stress is kept at 1 MPa. If the slope of the stress curve is large, fissures dramatically occur and spread horizontally in a short time, effects that are not beneficial for the stability control of the rocks with presplitting fissures.

Figures 5(b) and 5(c) show that the presplitting fissure intervals are 0.5 m and 1 m, which are short in distance. When mining to 0-6 m, the rock is weakened under the cutting action of rock formation. The presplitting fissures are not penetrated, so there is no momentary instability and the stress concentration is eased; stress around the presplitting fissures is 6-7 MPa, and its concentration factor is reduced to 1.1-1.3, which is better to ensure the integrity of its surrounding rock and fully engage the self-bearing rock capacity. When mining to 6-9 m, the tension stress among rocks in fractures overlaps to form an "O" ring with

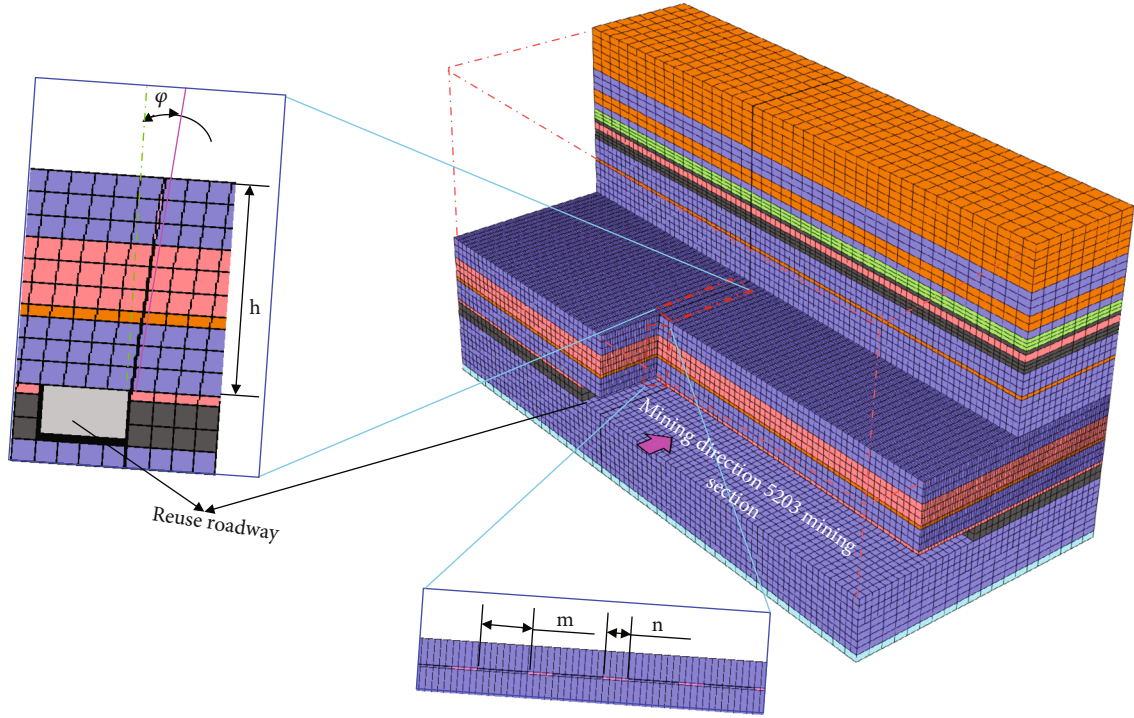


FIGURE 4: Numerical model of reused roadway.

TABLE 1: Physical and mechanical parameters of rock stratum.

Parameters	Bulk (GPa)	Shear modulus (GPa)	Tension (MPa)	Cohesion (MPa)	Friction ($^{\circ}$)	Density ($\text{kg}\cdot\text{m}^{-3}$)
Sand mudstone	12	8.6	2.1	1.2	32	2600
5# coal seam	1.5	2.0	1.2	0.9	24	2450
Mudstone	4.3	8.6	1.7	1.4	30	2200
Fine sandstone	36	12.6	7.2	1.45	31.5	2600
Siltstone	25	4.6	3.6	1.0	33	2500
2# coal seam	1.5	2.0	1.2	0.9	24	2450

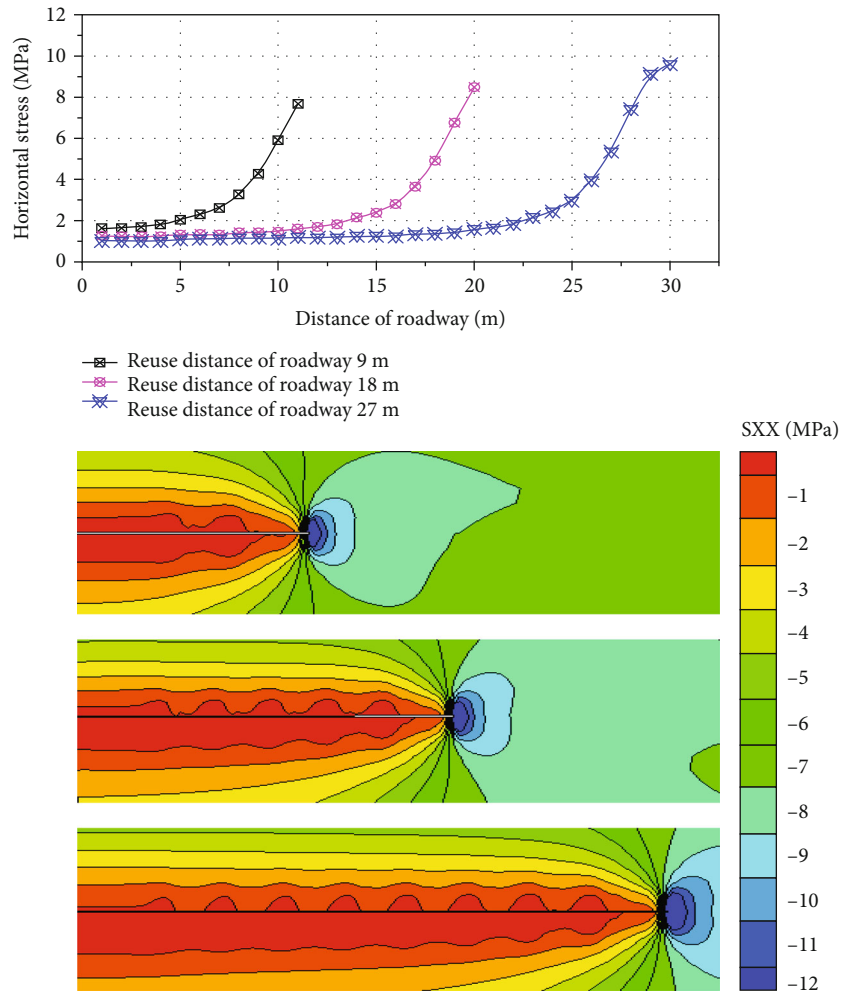
a radius of 0.5-1 m. The horizontal stress peak of rocks in the fissure interval reaches 10-12 MPa, and expansion and coalescence occur in the ends of the presplitting fissures. When mining to 9-12 m, the horizontal tensile stress starts to become stable, and the stability remains between 6 and 6.5 MPa. A large displacement occurs on the presplitting fissure in the short range, which benefits the timely caving of the compound soft rock formation, plugging of the gob side of the reused roadway, and rapid building of the reused roof cutting stowboard structure.

Figures 5(d) and 5(e) illustrate that the presplitting fissure intervals are 1.5 m and 2 m, and the distance between presplitting fissure interval rocks increases. When mining to 0-9 m, the control forces on both sides of the presplitting fissure become stronger. The horizontal tension stresses of both sides increase to 8-10 MPa, and the concentration factors are 1.45-1.8. The stress of the fractured interval rock is elliptical, and the stress concentrations at the fissure ends do not overlap. The central position of the horizontal tensile stress peak decreased to 8-9 MPa. When mining to 10-15 m, the horizontal displacement reaches its peak value, and the

slope of the stress curve is small and represents a cyclical fluctuation. The timely cutting effects of caving and plugging into the gob of the compound soft rock formation are not ensured, which influences the quick roadway construction effect.

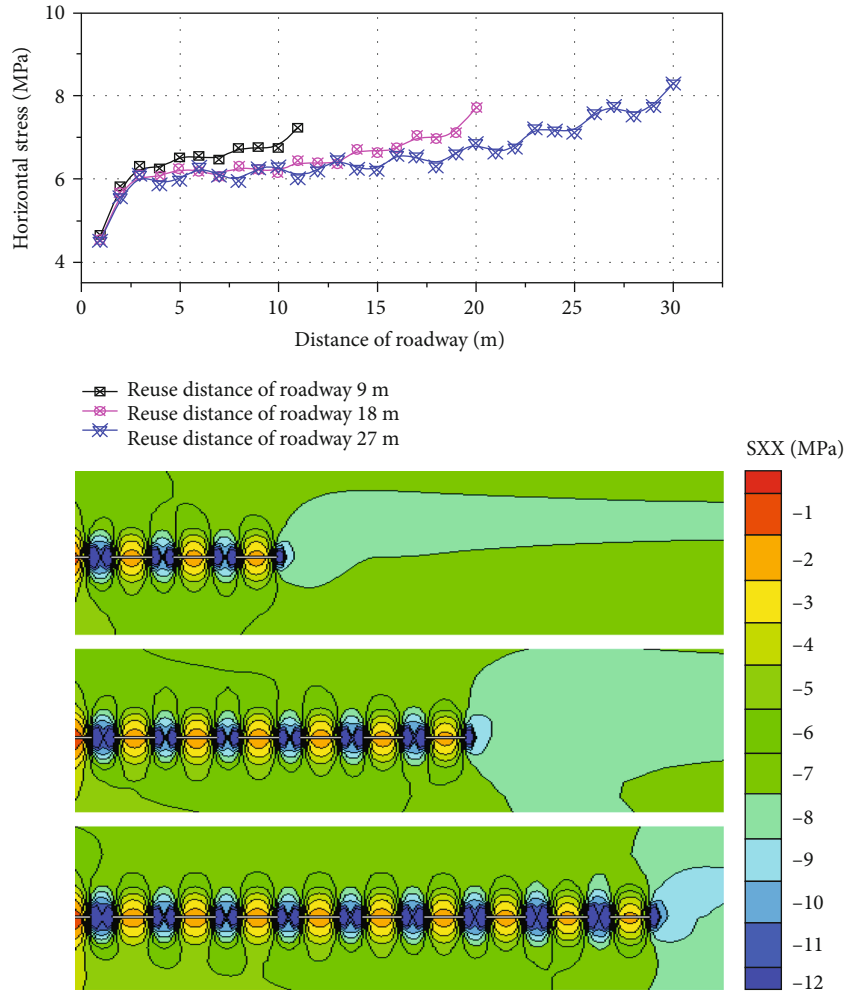
3.3. Plastic Damage Evolution Law of Presplitting Fissure Zones. As shown in Figure 6, in the vicinity of the fracture tip, the plastic zone is formed due to stress concentration and relaxation. Under mining disturbance action, the damage plastic zone is distributed along the axial direction of the reused roadway, the rock mass around the fracture decreased, and the plastic zone expanded.

As shown in Figure 6(a), the reused roadway is reserved and set as 0-9 m. Both sides of the fissure and the roof at the gob side are mainly shear damage. If 9-27 m is reserved, the shear stress is drastically attenuated from the peak, and frictional slip occurs between the fractures. Dilatancy displacement is restricted by the side, and the secondary fissure development is induced, which exacerbates the damage range of the fissure sidewall. In Figures 6(b) and 6(c), 0-



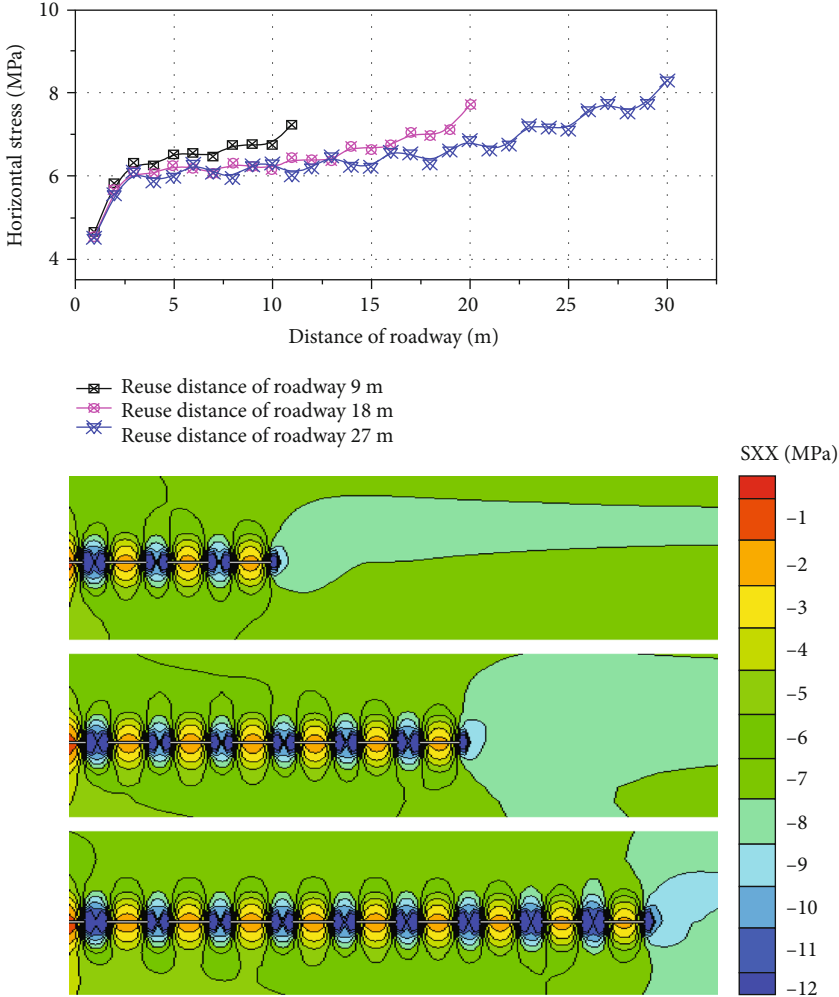
(a) Presplitting interval 0 m

FIGURE 5: Continued.



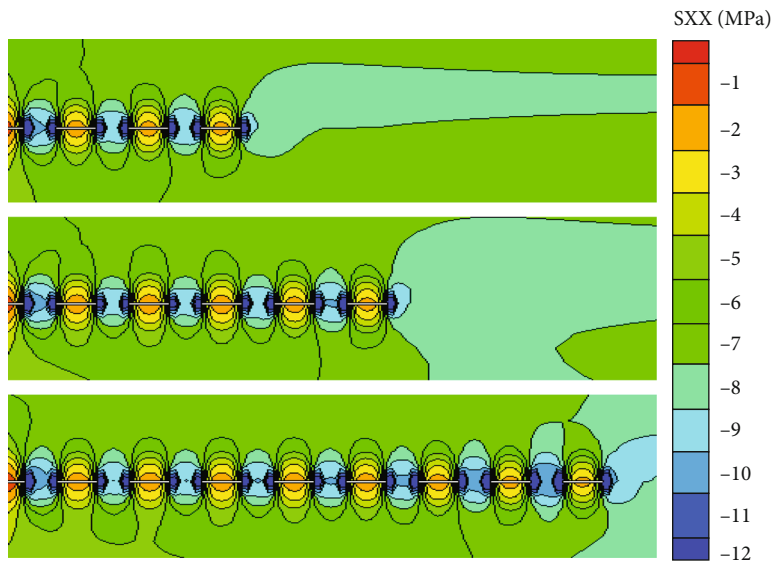
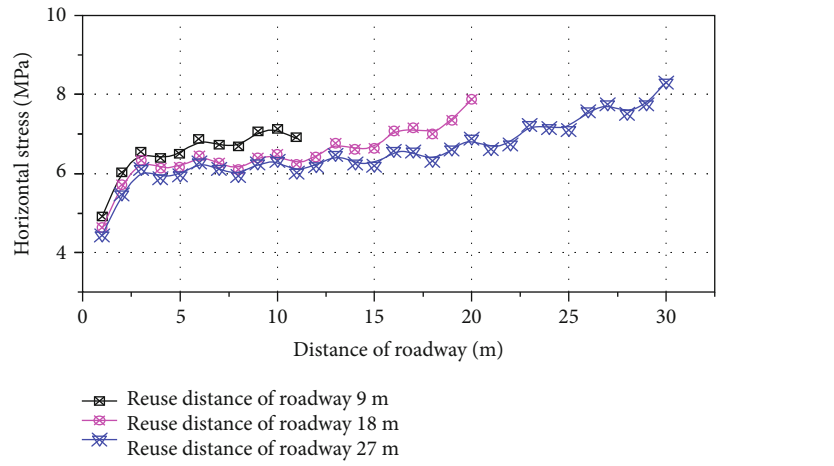
(b) Presplitting interval 0.5 m

FIGURE 5: Continued.



(c) Presplitting interval 1 m

FIGURE 5: Continued.



(d) Presplitting interval 1.5 m

FIGURE 5: Continued.

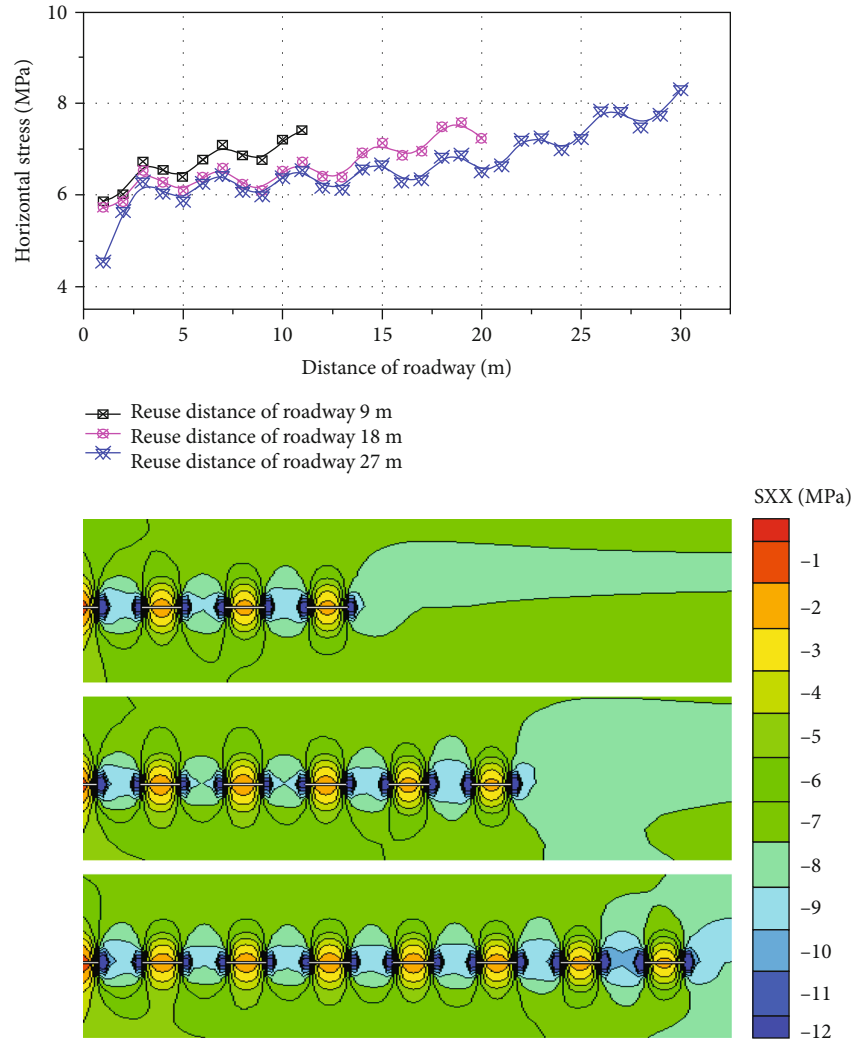
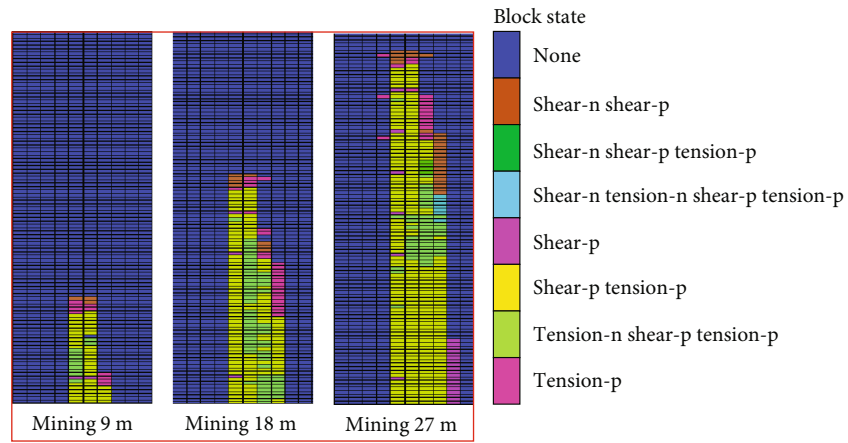


FIGURE 5: Horizontal tensile stress curve and stress nephogram of the presplitting zone.

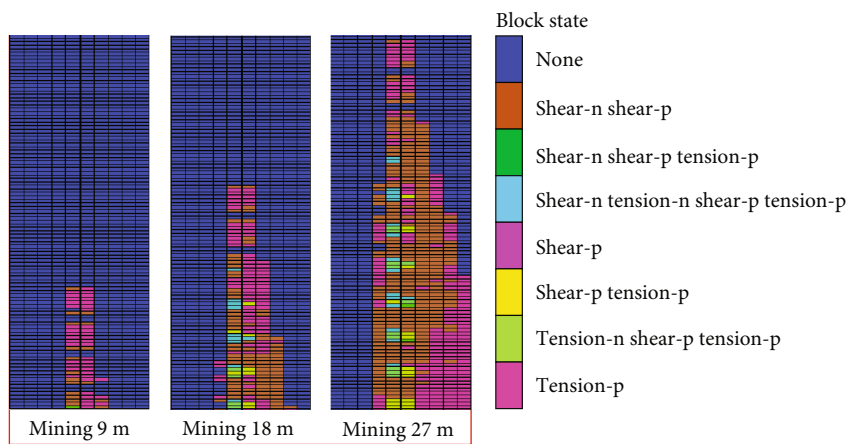
9 m is reserved in the reused roadway, and both sides of the fracture show damage. Due to the roof suspension area increase, the roof at the gob side is bent and sunken under the upper overlying stratum pressure and mining disturbance actions; the segregated rock is mainly subject to shear, and dilatant plastic damage occurs. When 0-18 m is reserved, the plastic area at both sides of the presplitting fissure has a sustainable development within 10 m from the initial end of the roadway. The force of the roof is from the shear stress to tension stress, the tensile and plastic damage areas increase, and the fissure interval accelerates the expanding and coalescence. The plastic areas are also connected to each other afterwards. When 27 m is reserved, the above evolution process proceeds in the roof presplitting fissures at the gob side; therefore, the expansion and coalescence cycle of its presplitting fissure is 8-10 m. In Figures 6(d) and 6(e), the fracture expansion is further limited when the presplitting fissure enlarges, and 0-18 m is reserved in the roadway. The suspension rock formation at the gob side does not experience large shear damage except

in the small area where shear dilation as well as tensile and plastic damages occurs; the presplitting fissure does not show an expansion trend. The retained roadway is 27 m. It reaches the intact cycle caving distance of the roof rock, and the overburden pressure is transferred to the compound soft rock formation. The roof shows dramatic bending, subsidence, instability, and collapse, and the presplitting fissure has large expansion and coalescence as well as shear dilation at the gob side. The tension and plastic damage areas intermingle. The presplitting fissure does not have a better control effect on the caving of the compound soft rock formation, and the expansion and coalescence cycle of the fissure reaches 18-25 m.

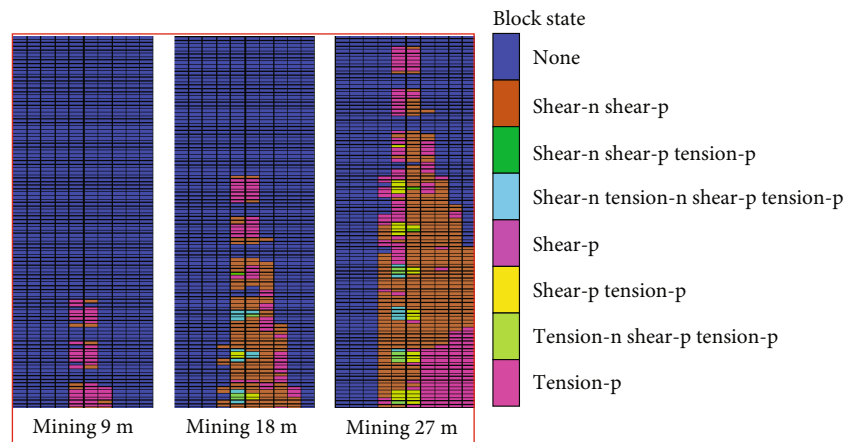
3.4. Energy Dissipation of Presplitting Fissure Features. Coal bump occurs in a very short period of time, and there is no sign before it occurs. In order to eliminate the occurrence of coal bump, many researches on the strain energy distribution characteristics were conducted. Energy is considered the internal variable through the presplitting fissure opening



(a) Presplitting interval 0 m



(b) Presplitting interval 0.5 m



(c) Presplitting interval 1 m

FIGURE 6: Continued.

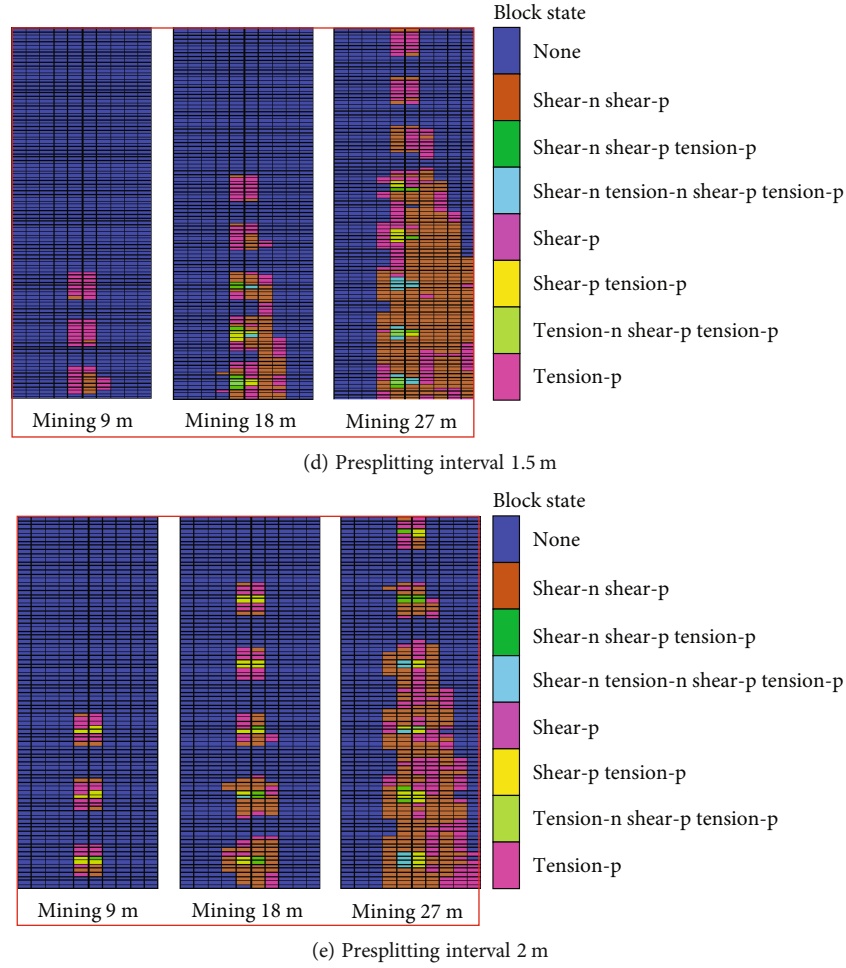


FIGURE 6: Plastic damage evolution process of rock mass in the presplitting area.

and spreading. The damage process of the surrounding rock damage and the evolution process can thus reflect the presplitting effect [26]. In the fracture propagation process, the energy is released at the fracture tip, part of which will be used to form a new fracture area, and the other produces plastic deformation. The energy release rate G of the presplitting fissure end region is greater than the surface free energy γ_s of the interval rock mass against fracture propagation, i.e., $G > \gamma_s$; the presplitting fissure will continue to expand and cross. According to the energy balance theory, the crack energy release rate G is as follows [27, 28]:

$$G = \frac{1}{2B} \frac{d(W - U)}{da}, \quad (8)$$

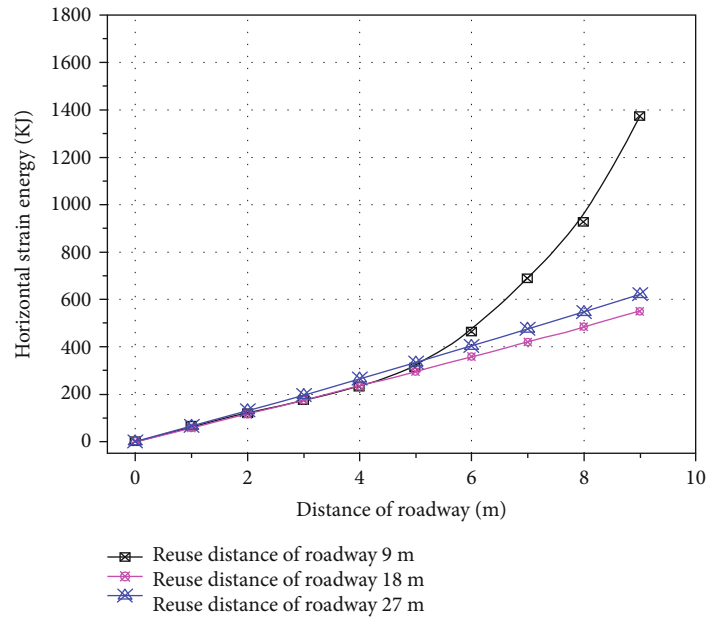
where W is external work done on the presplitting fissure structure, U is stored strain energy, B is thickness of the presplitting strata, and a is length of the presplitting fissure. According to Equation (8), when the strain energy U , the thickness of presplitting strata B , and the length of the presplitting fissure are certain, the presplitting fissure is subjected to the work W of the mining disturbed rock mass in

the horizontal direction as

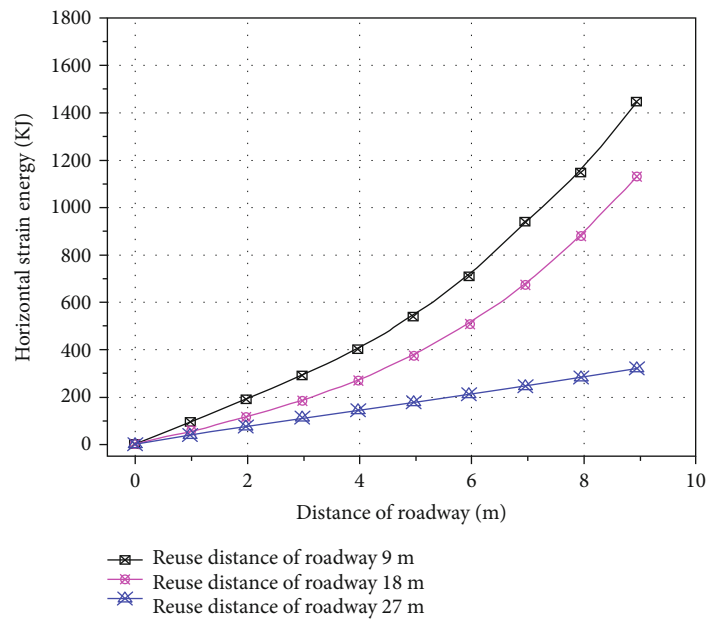
$$W = \int_l p(x)s(x)dx. \quad (9)$$

Monitoring lines are set in the gob side from the prefabricated fissure as 3 m. The horizontal tensile stress distribution $p(x)$ and the horizontal displacement $s(x)$ are fit into the polynomial equation and integrated into Equation (9), as shown in Figure 7. The dispersion curves of the strain energy dissipation in the horizontal direction of the fracture zone are then obtained.

The expansion and coalescence of a presplitting fissure are the exchange process of energy absorption, transformation, and release. As shown in Figure 7(a), when the retained roadway is 9 m, the slope of the curve becomes larger with the side roof of the gob cutting down along the fissure, and the sliding energy accelerates to release with a value of 1172.5 kJ. When the retained roadway is 18 m and 27 m, respectively, the curve changes from index variation to linear variation. The overlapping range of the upper and lower surfaces increases, which leads to the dilatancy effect. Large amounts of friction are created in

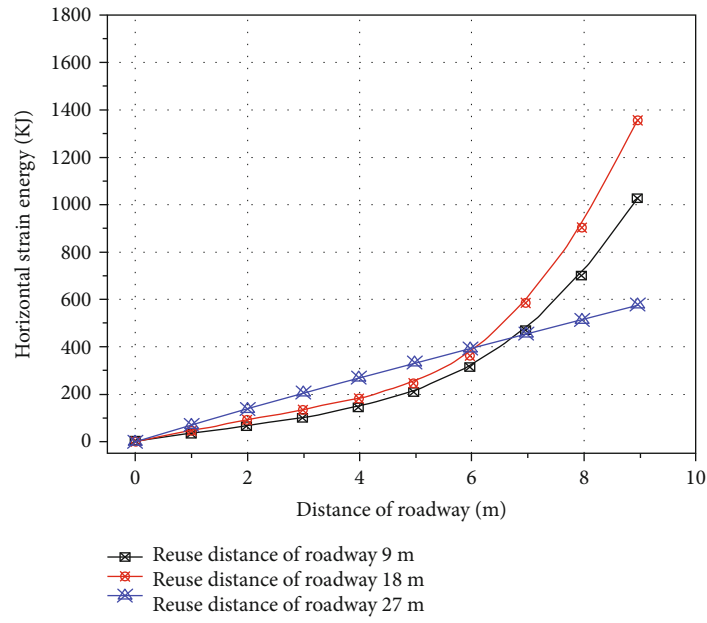


(a) Presplitting interval 0 m

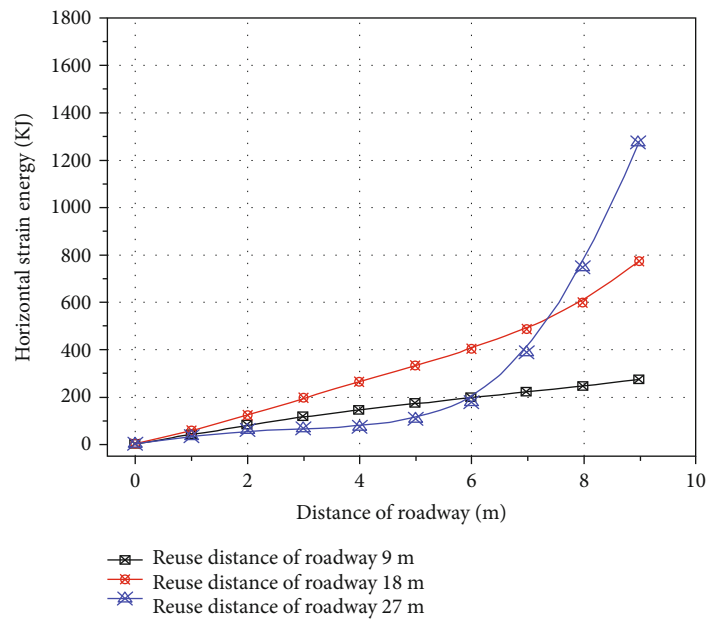


(b) Presplitting interval 0.5 m

FIGURE 7: Continued.



(c) Presplitting interval 1 m



(d) Presplitting interval 1.5 m

FIGURE 7: Continued.

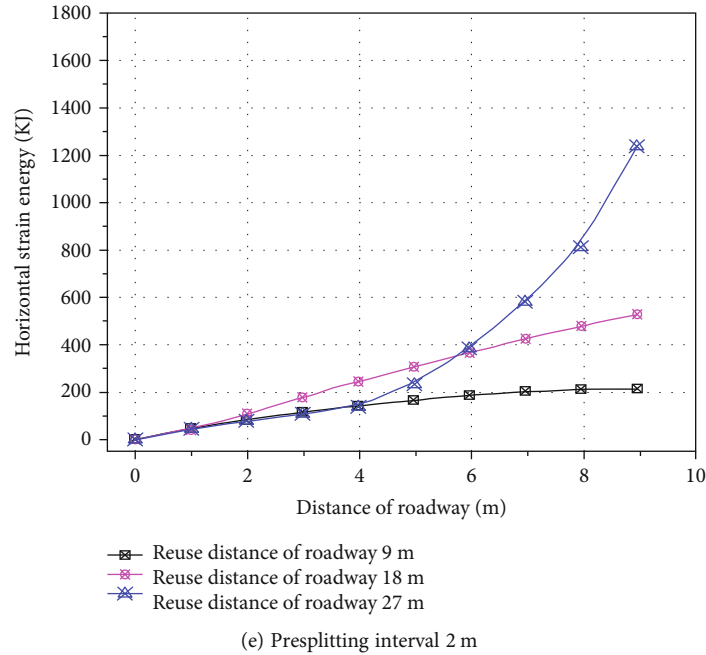


FIGURE 7: Strain energy accumulation and dissipation curve of presplitting fissure propagation.

the gap interfaces, and the energy consumption rate decreases to 550 kJ, which is 47% of the initial rate. In Figures 7(b) and 7(c), the retained roadway is 0-18 m, and the presplitting fissure remains in a stable expansion stage while the elastic strain energy release curve presents an exponential form and steady growth. The strain energy of the rocks around the presplitting fissure has sustainable growth, and the average peak value reaches 1,650 kJ when the retained roadway is 9-18 m. At this point, the accumulated ability of the elastic strain energy release reduces because the initial fissure occurs. When the retained roadway is 27 m, the fissures continually expand and link, so the energy consumption rate of the surface shows a linear increase. Meanwhile, the peak values decrease to 319 kJ and 576 kJ, which are 19.3% and 32.7% of the peak, respectively, and the shear friction weakens and quickly achieves that of the stowboard. In Figures 7(d) and 7(e), no cutting downward or sinking occurs along the presplitting fissure of the soft rock formation at the gob side. However, the overall bending subsidence occurs based on the solid roadway rock. When the retained roadway is 9 m, the plastic deformation of the solid rock is large, the strain energy rapidly accumulates, the broken rock zone of the surrounding roadway rock is enlarged, and the elastic strain energy release decreases to a peak value of 1,100 kJ. Compared with the presplitting fissure intervals of 0.5 m and 1 m, the slope of the curve flattens and decreases greatly to 66%, seriously weakening the fracture expansion capacity. When the retained roadway is 9-27 m, the elastic strain energy curve presents a linear variation, of which the mean peak value is 360 kJ. The energy consumption rate decreases, and the linkage cycle period is prolonged, causing difficulties in achieving quick stowboard after mining.

4. Analysis on the Stability of Roadway

4.1. Deformation and Plastic Damage Characteristics of Surrounding Roadway Rock. Rocks have strain softening and dilatancy characteristics. The failure zone of the surrounding rocks is the cause of increased pressure and deformation of the surrounding rock [29, 30]. In reused roadways, during the initial excavation process, the medium-term mining disturbance, and the latter part of the maintenance and reuse process, the elasticity, plasticity, and rupture of the surrounding rock have an evolutionary process. The occurrence, development, and stability generally cause an unstable state of destruction. The larger the damage area is, the greater the amount of convergence deformation is [31]. Therefore, the size of the surrounding rock damage rupture zone is a measure of the degree of instability of the surrounding rock key factors.

As shown in Figure 8, the presplitting fissure interval is 0 m and 0.5 m, since the lateral diastrophism limit of the compound soft rock formation is greatly weakened, and the fissure interfaces overlap during collapse, the rock integrity is destroyed, and the bearing capacity is weakened. The friction action between the interfaces enlarges the shear and plastic damage around the fissures, which easily leads to a rapid collapse due to the sudden instability on the side rock mass of the reused roadway. The upper stable rock suddenly loses the support of the lower rock to create a stress concentration and a large range of tension damage occurs. The 1 m presplitting fissure weakens the flexural rigidity of the roadway soft rock mining side as a tensile fracture. The falling rock formation inversion alleviates the dilation friction between fractures. Meanwhile, the plastic zone of the roadway gob side soft rock formation has a wedge distribution with a large end towards the bottom, which is advantageous

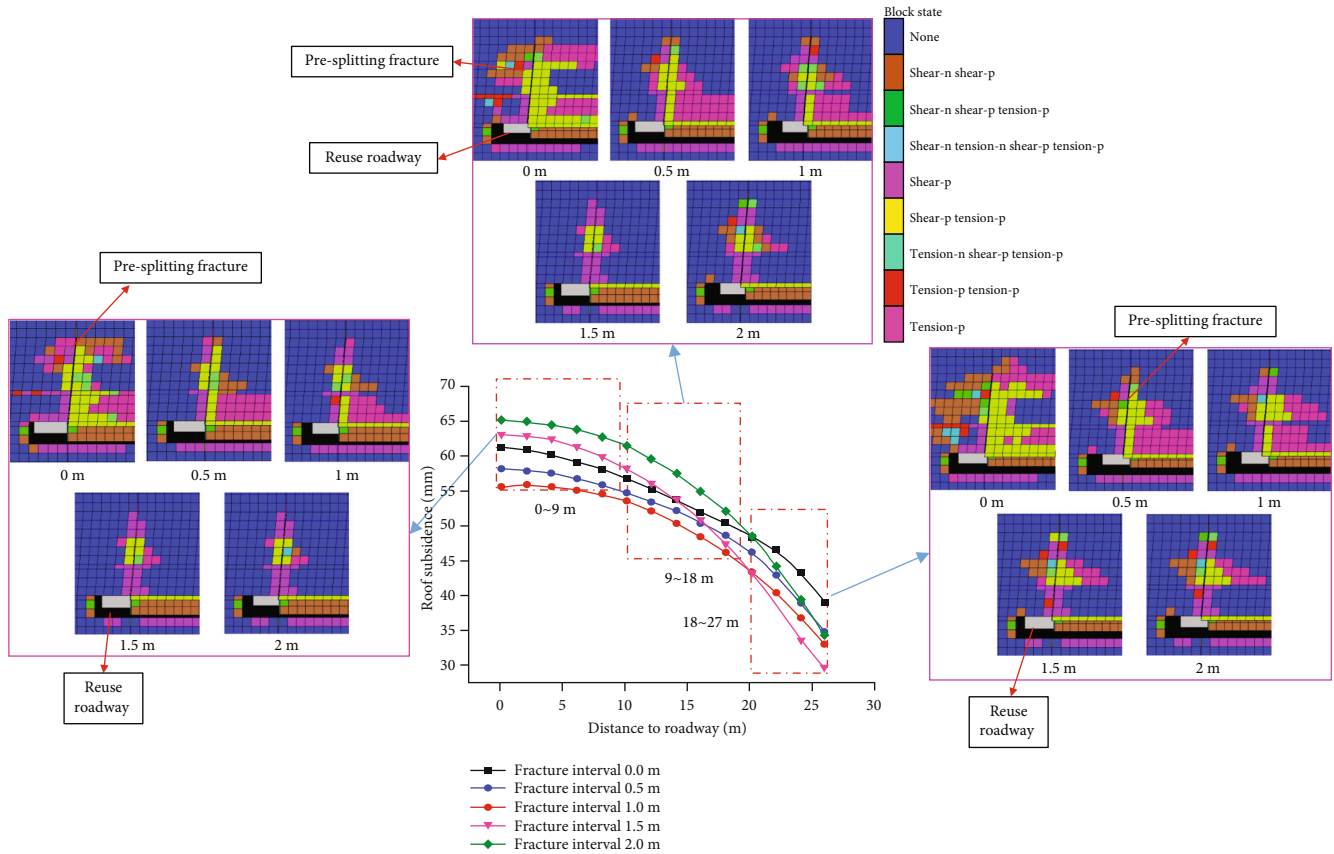


FIGURE 8: Deformation curves and plastic damage distribution characteristics of surrounding reused roadway rock.

for the successive, coordinated caving of low and median rock formations. A stable supporting structure at the gob side of roadway is then formed. In the case of presplitting fissure intervals of 1.5 m or 2 m, the fracture effect will slightly weaken the flexural rigidity of the rock formation, with the roofs of both sides being sidewise limited. The compound rock formation is not easily cut downwards along the pre-splitting fissure, resulting in the whole roadway tilting down sharply and going against the stability of surrounding rocks.

4.2. Study on the Roadway Roof Stratum Stability. One side of the reused roadway is the solid coal, and the other side is the filling body. The roof deformation is asymmetric, so the roof to the gob side rotation subsides, and the roof above the gob produces a wide range of shear failure. Thin, weak, soft rocks exist in the overlying roadway strata, the stratum movement is severe, and the shear slip range and tear propagation increase [32]. The roof separation and separation stratum increases cause the bearing capacity of the rock stratum to be greatly reduced, which threatens the stability of the surrounding rock. The upper roadway section of 10 m is the cut-off section of the pre-splitting fracture. The distribution range of the composite soft rock, the presplitting cracks on the upper reused roadway at 10 m, and the composite soft rock distribution influence the stability of the surrounding rock. As shown in Figure 8, the distribution curve of the upper 3 m, 6 m, and 9 m shows vertical stress.

Different interrock formation properties including the stiffness, intensity, and joint development occur in the structural plane and are prone to separation under high stress. According to the comprehensive geological histogram, the upper sections that are 3 m and 6 m higher than the roadway are composed of thick and well-bearing sandy mudstone and mudstone; sections 9 m higher than the road are close to the upper section of the compound soft rock, which is adjacent to the upper stable rock. Upper, lower, and middle rocks are mingled with several types of soft rock strata, making it prone to separation and instability. Figures 9(a) and 9(b) show that with an increase in retained roadway distance, the 3 m and 6 m high rock formations are close to the gob side. The vertical slope of the vertical stress curve increases, and the sloping deformation is obvious on the gob side; the shear slippage on the structural plane is intense. The shear stress increases as its distance away from the solid coal seam of roadway increases, resulting in an increase in local curvature and the formation of an isolated instability zone. A vertical stress of 9 m high rock appears high in the middle and bottom of both ends. Deflection appears when bending, and the maximum vertical stress reaches 10.3 MPa and 7.6 MPa at the gob side. The rock section is in a nonlinear state of rotation, buckling, etc., which leads to the separation and instability of the upper stable roadway rock. In Figure 9(c), the average change in the vertical stress range of the 3 m, 6 m, and 9 m high rocks is smaller. The deformation deflection remains consistent, and coordinated roof deformation

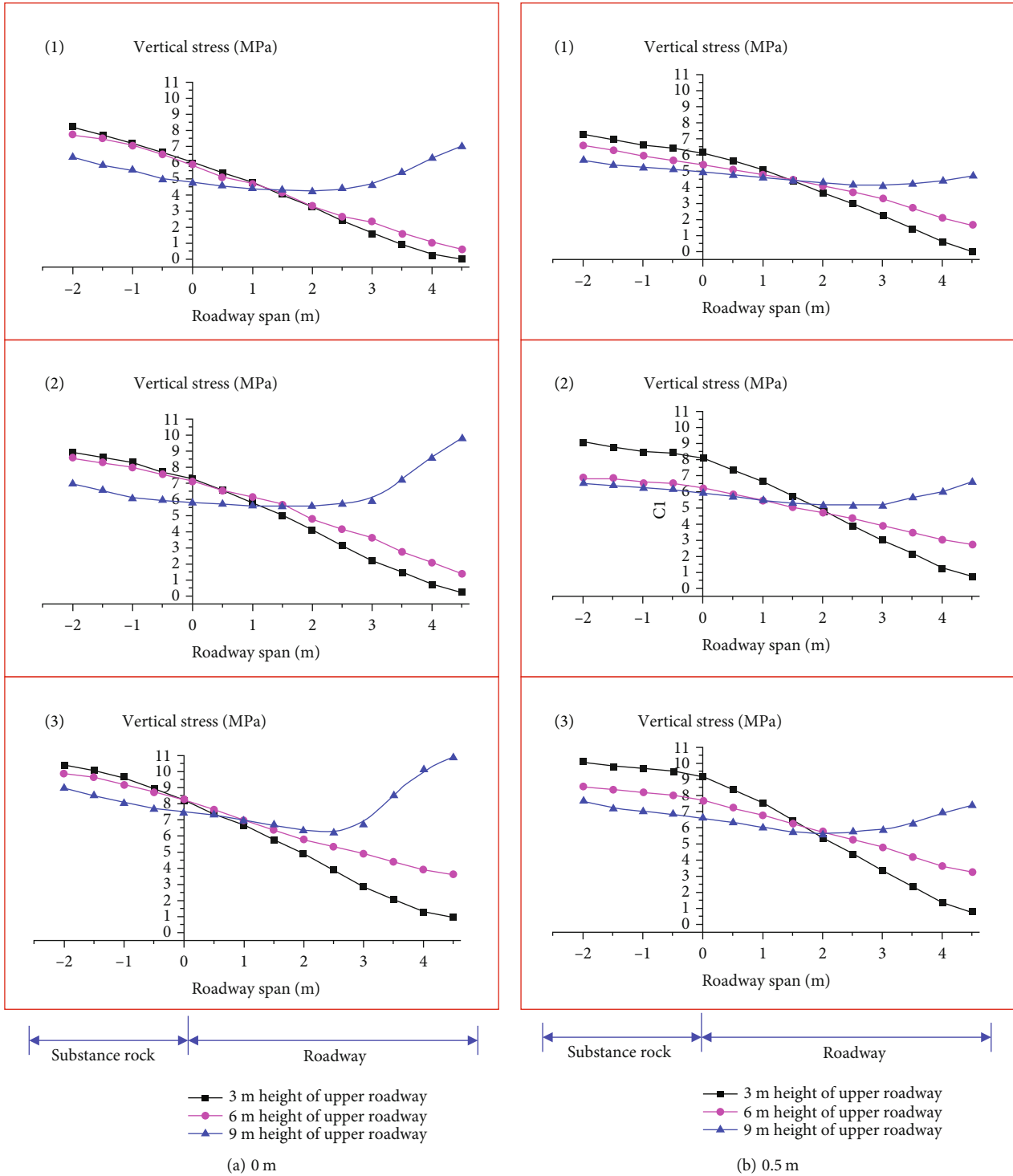


FIGURE 9: Continued.

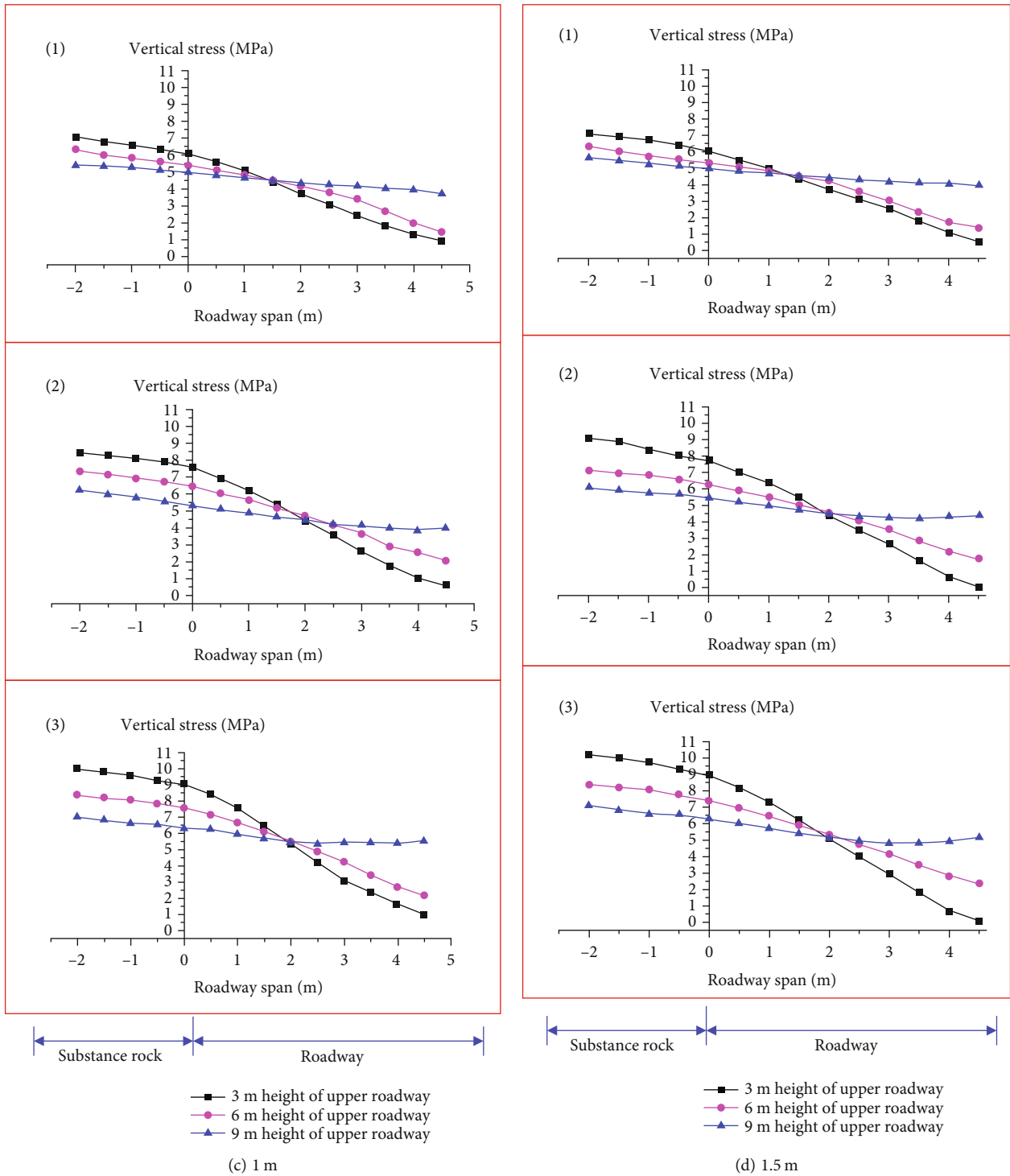


FIGURE 9: Continued.

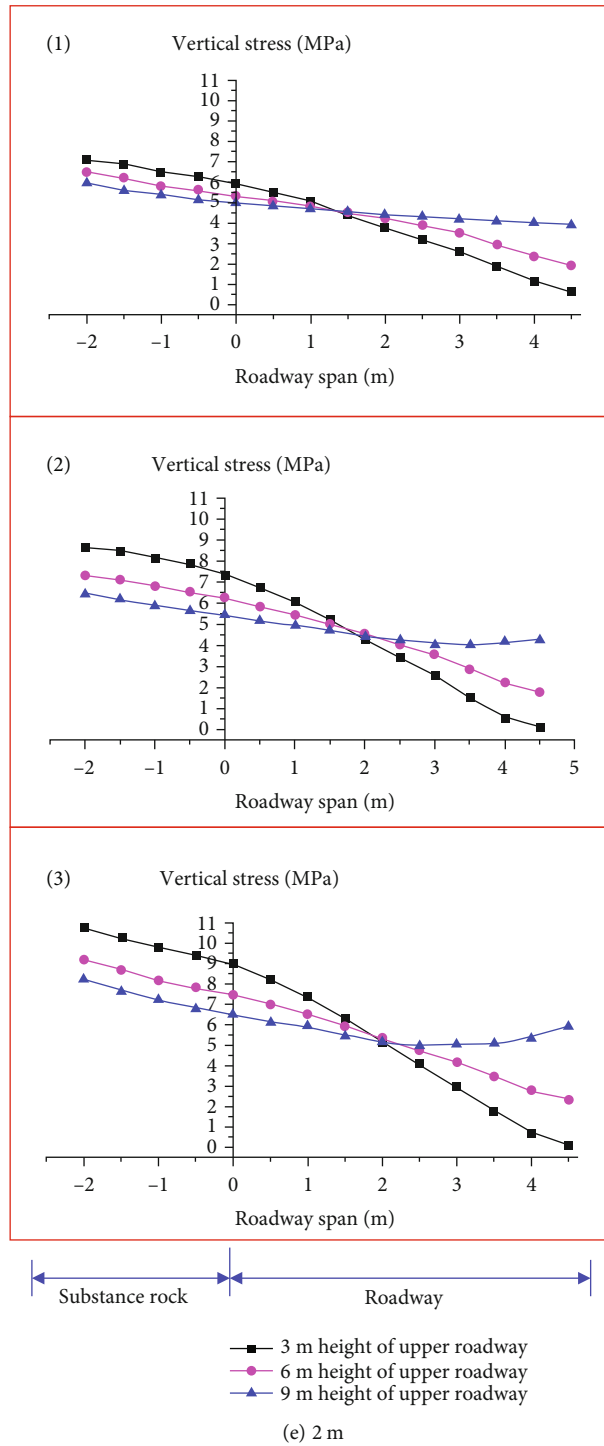


FIGURE 9: Stress distribution of the Reused roadway roof at the heights of (1) 9 m, (2) 18 m, and (3) 27 m.

develops, restricting the separation and dislocation of the rock formation surface and assuring the integrity of the compound soft rock and the stability of the surrounding roadway rocks. Therefore, the stress concentration weakened, and the pressure change eased. In Figures 9(d) and 9(e), the vertical stresses of the gob and solid coal-rock sides of the 3 and 6 m high rock formations decrease and increase, respectively; as increasing gap of the retained roadway

increases, the vertical stress difference on both sides increases sharply, and the roadway roof stress concentration coefficient is larger, increasing the shear slip and immediately tearing the fissure growth at the two ends of the 9 m rock formation and structural plane. The separation range of the middle section of the structural plane is enlarged and is prone to local separation and instability, making it difficult to maintain the surrounding roadway rock.

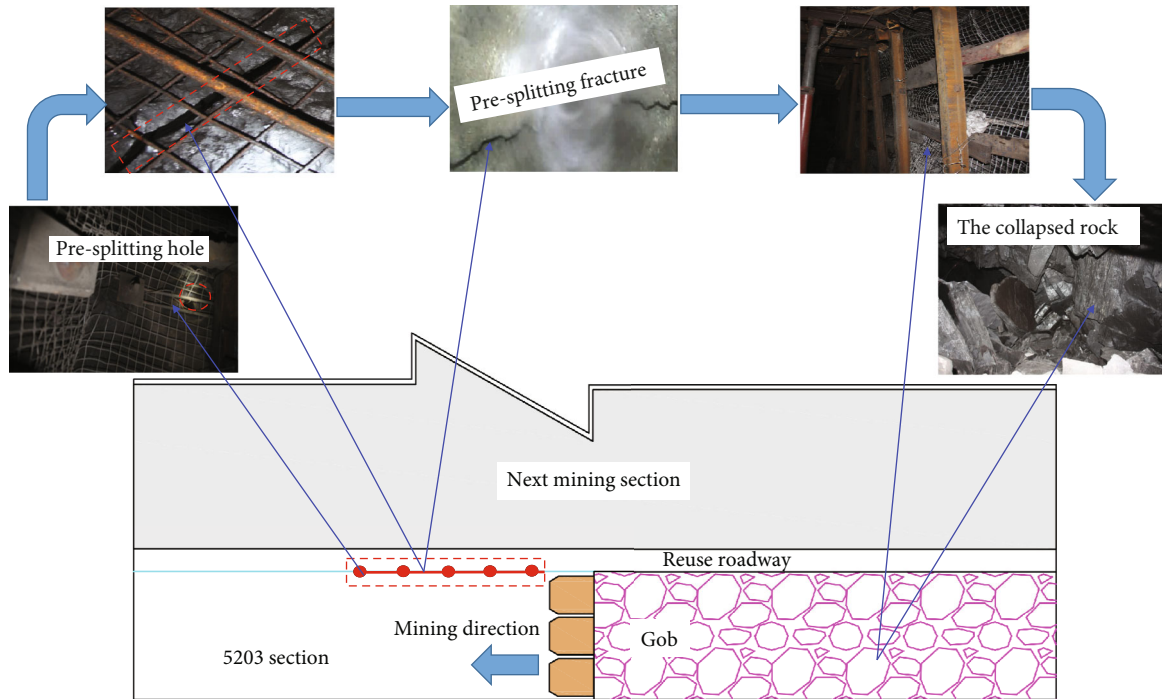


FIGURE 10: Expansion and penetration field test of roof presplitting fractures.

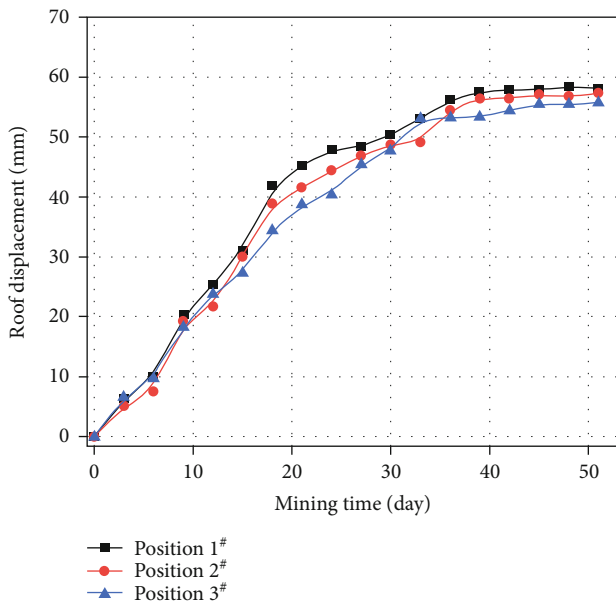


FIGURE 11: Deformation law of roadway roof.

5. Field Test

Based on the simulation results, the optimal presplitting interval of roof is 1 m. In field test, the roof presplitting line could be arranged at about 1 m from the presplitting side of the roadway roof and the purpose is to facilitate the construction of drilling equipment. At the same time, it is also convenient to maintain the integrity of reused roadway surrounding rock. The presplitting interval 1 m of roof fracture is implemented in the field test, as shown in Figure 10. The



FIGURE 12: The stable reused roadway surrounding rock after roof presplitting.

whole process of the formation, development of the presplitting cracks, and the deformation of the overlying strata is observed by the method of drilling.

In front of the mining work, the roof of the reused roadway is presplitting fractures. Behind the mining working face of 0~3.0 m, the fractures appear on the roof of the roadway and finally connect each other and begin to fall. Behind the mining working face of 3.0~6.0 m, the upper strata show coordinated deformation. Compound soft rock strata fall and plug fully at the gob side to form the reused roadway structure. Through drilling observation, there is no obvious separation and dislocation; the roof rock is more complete. Three deformation monitoring stations are arranged in the roadway, each 50 m apart. After mining face for 40 days, the deformation of roadway roof is effectively controlled and surrounding rock tends to be stable, as shown in Figures 11 and 12.

6. Conclusions

- (1) Based on the engineering needs of compound soft rock, the characteristics of overlying stratum mechanisms, presplitting, extension, and coalescence of rock formation are examined. The compound soft rock stratum breaking and falling process is established, and the dynamic pressure of the upper strata causes the rapid pressurization and collapse of the support structure. This is one of the key factors affecting the stability of the surrounding rock of reused roadways
- (2) A three-dimensional model with fissure interval conditions of 0 m, 0.5 m, 1 m, 1.5 m, and 2 m is established to analyze the horizontal stress around the presplitting fissure, the plastic damage evolution rule, and energy dissipation features associated with fissure extension. In the case of presplitting fissure intervals of 0.5 m and 1 m, the stress concentration of the initial section of the retained roadway is removed, and the presplitting fissure is expanded and cut through, effectively controlling the dilatancy and damage of the surrounding rock mass and the energy dissipation process. This control is also beneficial to the coordinated caving of rock formations
- (3) When the presplitting fissure interval is 1 m, the stress transfer caused by mining disturbance is obstructed and the flexural rigidity of side soft rock formation of roadway mining side is weakened. By avoiding the dilatancy friction, the plastic zone of the roadway gob side weak strata has a wedge distribution with the big end down, which is advantageous for the successive, coordinated caving of low and median rock formations. This type of caving limits the separation and dislocation of the roadway roof rock surface and helps to form a stable supporting structure on the gob side of the roadway and increases the self-bearing capacity of the upper rocks
- (4) A 1 m presplitting fissure interval is adopted to be used in field test and on the monitoring surface: if the reused roadway is reserved and set as 3–6 m, the presplitting fissures will connect. If the reused roadway is reserved and set as 9–12 m, the roadways will be constructed after being plugged and cut downwards along the coalescence fractured from top to bottom. After mining 40 days, the surrounding rock deformation of reused roadway tends to be steady

Data Availability

The data used to support the findings of this study are included within the article.

Conflicts of Interest

The authors declare that they have no conflicts of interest.

Acknowledgments

This study was supported by the National Natural Science Foundation of China (No. 52104157) and Funding Program of Research Projects in Henan Province (No. 222102320239).

References

- [1] S. Q. Yang, M. Chen, G. Fang et al., “Physical experiment and numerical modelling of tunnel excavation in slanted upper-soft and lower-hard strata,” *Tunnelling and Underground Space Technology*, vol. 82, pp. 248–264, 2018.
- [2] B. Lin, F. Yan, C. Zhu et al., “Cross-borehole hydraulic slotting technique for preventing and controlling coal and gas outbursts during coal roadway excavation,” *Journal of Natural Gas Science and Engineering*, vol. 26, pp. 518–525, 2015.
- [3] J. Ning, J. Wang, X. Liu, K. Qian, and B. Sun, “Soft-strong supporting mechanism of gob-side entry retaining in deep coal seams threatened by rockburst,” *International Journal of Rock Mechanics and Mining Sciences*, vol. 24, no. 6, article S2095268614001463, pp. 805–810, 2014.
- [4] J. Wang, J. Zhang, and Z. Li, “A new research system for caving mechanism analysis and its application to sublevel top-coal caving mining,” *International Journal of Rock Mechanics and Mining Sciences*, vol. 88, pp. 273–285, 2016.
- [5] W. S. Xu, W. T. Xu, and Y. H. Cheng, “Research on the reasonable strengthening time and stability of excavation unloading surrounding rock of high-stress rock mass,” *Geofluids*, vol. 2021, Article ID 3508661, 2021.
- [6] B. Wang, F. Dang, S. Gu, R. Huang, Y. Miao, and W. Chao, “Method for determining the width of protective coal pillar in the pre-driven longwall recovery room considering main roof failure form,” *International Journal of Rock Mechanics and Mining Sciences*, vol. 130, p. 104340+11, 2020.
- [7] Y. L. Tan, F. H. Yu, J. G. Ning, and T. B. Zhao, “Design and construction of entry retaining wall along a gob side under hard roof stratum,” *International Journal of Rock Mechanics and Mining Sciences*, vol. 77, article S1365160915000842, pp. 115–121, 2015.
- [8] J. X. Yang, C. Y. Liu, B. Yu, and F. F. Wu, “The effect of a multi-gob, pier-type roof structure on coal pillar load-bearing capacity and stress distribution,” *Bulletin of Engineering Geology and the Environment*, vol. 74, no. 4, article 685, pp. 1267–1273, 2015.
- [9] Y. Fan, W. Lu, Y. Zhou, P. Yan, Z. Leng, and M. Chen, “Influence of tunneling methods on the strainburst characteristics during the excavation of deep rock masses,” *Engineering Geology*, vol. 201, pp. 85–95, 2016.
- [10] H. Zhu, B. Ye, Y. Cai, and F. Zhang, “An elasto-viscoplastic model for soft rock around tunnels considering overconsolidation and structure effects,” *Computers and Geotechnics*, vol. 50, pp. 6–16, 2013.
- [11] Y. J. Wang, Y. B. Gao, E. Y. Wang, M. He, and J. Yang, “Roof deformation characteristics and preventive techniques using a novel non-pillar mining method of gob-side entry retaining by roof Cutting,” *Energies*, vol. 11, no. 3, pp. 627–630, 2018.
- [12] D. W. Yang, Z. G. Ma, F. Z. Qi et al., “Optimization study on roof break direction of gob-side entry retaining by roof break and filling in thick-layer soft rock layer,” *Geomechanics and Engineering*, vol. 13, pp. 195–215, 2017.

- [13] R. Gu and U. Ozbay, "Numerical investigation of unstable rock failure in underground mining condition," *Computers and Geotechnics*, vol. 63, pp. 171–182, 2015.
- [14] X. L. Yang, J. S. Xu, Y. X. Li, and R. M. Yan, "Collapse mechanism of tunnel roof considering joined influences of nonlinearity and non-associated flow rule," *International Journal of Geomechanics Engineering*, vol. 10, no. 1, pp. 21–35, 2016.
- [15] Y. Yong, S. Tu, X. Zhang, and L. Bo, "Dynamic effect and control of key strata break of immediate roof in fully mechanized mining with large mining height," *Shock and Vibration*, vol. 2015, Article ID 657818, 11 pages, 2015.
- [16] X. Li, M. Ju, Q. Yao, J. Zhou, and Z. Chong, "Numerical investigation of the effect of the location of critical rock block fracture on crack evolution in a gob-side filling wall," *Rock Mechanics and Rock Engineering*, vol. 49, no. 3, pp. 1041–1058, 2016.
- [17] H. G. Ji, H. S. Ma, J. A. Wang, Y. H. Zhang, and H. Cao, "Mining disturbance effect and mining arrangements analysis of near-fault mining in high tectonic stress region," *Safety Science*, vol. 50, no. 4, pp. 649–654, 2012.
- [18] X. Li and W. Li, "Numerical investigation on fracturing behaviors of deep-buried opening under dynamic disturbance," *Tunnelling and Underground Space Technology*, vol. 54, pp. 61–72, 2016.
- [19] Y. Li, D. Zhang, Q. Fang, Q. Yu, and L. Xia, "A physical and numerical investigation of the failure mechanism of weak rocks surrounding tunnels," *Computers and Geotechnics*, vol. 61, pp. 292–307, 2014.
- [20] B. X. Huang, Q. Y. Cheng, X. L. Zhao, W. Xue, and M. Scoble, "Using hydraulic fracturing to control caving of the hanging roof during the initial mining stages in a longwall coal mine: a case study," *Arabian Journal of Geosciences*, vol. 11, no. 20, pp. 603–618, 2018.
- [21] F. Z. Qi and Z. G. Ma, "Investigation of the roof presplitting and rock mass filling approach on controlling large deformations and coal bumps in deep high-stress roadways," *Latin American Journal of Solids and Structures*, vol. e190, pp. 1–24, 2019.
- [22] B. X. Huang, Y. Z. Wang, and S. G. Cao, "Cavability control by hydraulic fracturing for top coal caving in hard thick coal seams," *International Journal of Rock Mechanics and Mining Sciences*, vol. 74, pp. 45–57, 2015.
- [23] C. Periasamy and H. V. Tippur, "Measurement of crack-tip and punch-tip transient deformations and stress intensity factors using Digital Gradient Sensing technique," *Engineering Fracture Mechanics*, vol. 98, pp. 185–199, 2013.
- [24] J. B. Bai, W. L. Shen, G. L. Guo, X. Y. Wang, and Y. Yu, "Roof deformation, failure characteristics, and preventive techniques of gob-side entry driving heading adjacent to the advancing working face," *Rock Mechanics and Rock Engineering*, vol. 48, no. 6, pp. 2447–2458, 2015.
- [25] W. L. Tian and S. Q. Yang, "Experimental and numerical study on the fracture coalescence behavior of rock-like materials containing two non-coplanar filled fissures under uniaxial compression," *Geomechanics and Engineering*, vol. 12, no. 3, pp. 541–560, 2017.
- [26] G. F. Wang, S. Y. Gong, Z. L. Li, L. M. Dou, W. Cai, and Y. Mao, "Evolution of stress concentration and energy release before rock bursts: two case studies from Xingan coal mine, Hegang, China," *Rock Mechanics and Rock Engineering*, vol. 14, pp. 1–9, 2016.
- [27] H. Zhou, C. K. Qu, D. W. Hu et al., "In situ monitoring of tunnel deformation evolutions from auxiliary tunnel in deep mine," *Engineering Geology*, vol. 221, article S0013795217302247, pp. 10–15, 2017.
- [28] N. Falaknaz, M. Aubertin, and L. Li, "Numerical analyses of the stress state in two neighboring stopes excavated and back-filled in sequence," *International Journal of Geomechanics*, vol. 15, no. 6, p. 04015005, 2015.
- [29] H. Yan, F. He, T. Yang, L. Li, S. Zhang, and J. Zhang, "The mechanism of bedding separation in roof strata overlying a roadway within a thick coal seam: a case study from the Pingshuo Coalfield, China," *Engineering Failure Analysis*, vol. 62, pp. 75–92, 2016.
- [30] G. R. Feng, P. F. Wang, and Y. P. Chugh, "Stability of gate roads next to an irregular yield pillar: a case study," *Rock Mechanics and Rock Engineering*, vol. 52, no. 8, pp. 2741–2760, 2019.
- [31] W. Feng, R. Huang, and T. Li, "Deformation analysis of a soft-hard rock contact zone surrounding a tunnel," *Tunnelling and Underground Space Technology*, vol. 32, pp. 190–197, 2012.
- [32] S. Zhang, D. S. Zhang, H. Z. Wang, and S. S. Liang, "Discrete element simulation of the control technology of large section roadway along a fault to drivage under strong mining," *Journal of Geophysics and Engineering*, vol. 15, no. 6, pp. 2642–2657, 2018.